Using NEMOH for Modelling Wave Energy Converters: A Comparative Study with WAMIT

Markel Penalba[1], Thomas Kelly[2] and John V. Ringwood[3]
Centre for Ocean Energy Research (COER), Maynooth University, Co.Kildare, Ireland
markel.penalbaretes.2015@mumail.ie[1]
thomas.e.kelly.2012@mumail.ie[2]
john.ringwood@nuim.ie[3]

***Abstract*—Despite the well-known limitations of linear potential flow theory, hydrodynamic coefficients obtained from boundary element methods (BEM) are commonly used to estimate the hydrodynamic parameters of wave energy converters (WECs). These parameters may then be used to simulate the behaviour of WECs in response to incident waves. In this work, the usefulness to the wave energy community of the open-source BEM solver, NEMOH, developed by the École Centrale de Nantes, is independently considered by comparison with the commercially-available BEM solver, WAMIT. The pre-processing, processing and post-processing stages of analysing four typical wave energy converting concepts are considered. Results for both solvers are presented in both the frequency and time domains. Other issues considered include computational time taken by both solvers, mesh generation, user-friendliness and the availability of supporting documentation.**

***Index Terms*—Wave energy, boundary element method solvers, WAMIT, NEMOH, hydrodynamic coefficients**

I. Introduction

Techniques to numerically simulate the behaviour of WECs in response to ocean waves are critical to the development of a wave energy industry. Numerical models may be used to predict the motions of, forces acting on and power output from a WEC. Such models may also be used as input to power take-off system models, proposed control strategy models, and financial models. Obtaining results from numerical modelling is typically significantly less expensive than deriving the equivalent results from physical scale models using tank testing. BEM is perhaps the most common method used in the wave energy context. While limited by the linear nature of potential flow theory, the speed with which numerical simulation may be performed when compared to other simulation methods, such as computational fluid dynamics (CFD) or smoothed-particle hydrodynamics (SPH), makes BEM a common choice for early-stage device development.

In this paper, a comparison is made between key device parameters, for a number of typical WEC concepts, obtained using the well-established, commercial BEM solver, WAMIT, and a recently-released, open-source BEM solver, NEMOH. BEM techniques are first introduced. A number of commercial BEM solvers are presented, as is the open-source solver. The relative usage by the wave energy community of each solver is estimated based on a survey of the number of references to each solver in the *Proceedings of the 11th European Wave and Tidal Energy Conference* [1]. This survey provided the rationale for considering WAMIT as the commercial solver of choice. Further, the choice of which four WEC concepts to compare is also informed by this survey.

WAMIT and NEMOH are then compared under three headings. Firstly, the pre-processing stage for both solvers is compared with regard to the user interface, available documentation and user-friendliness of pre-processing. Particular regard is given to the means by which the geometry under analysis is described through a process of mesh generation.

Secondly, the processing stage, wherein the solver analyses the geometry in question, is compared for the two solvers. A comparison between the key parameters obtained by the processors for the four WEC concepts considered in both the frequency and time domains are presented in graph and tabular form. Further, consideration is also given to the processing time required by each solver. In the final stage of the study, the use of the results from both solvers with third party post-processors is compared.

The paper concludes with a discussion of the benefits and disadvantages of the use of both solvers for the analysis of different WEC concepts, as determined during this study.

II. Boundary Element method

BEM, also known as the panel method, is a numerical technique which uses systems of partial differential equations formulated into the boundary integral form. BEM codes employ the method of Green's functions to transform a flow problem into a problem of source distribution on the body surface [3]. BEM codes may be applied to varying engineering problems, and when used in a hydrodynamic context, BEM is used to solve for the scatter and radiated velocity potentials, which are solved separately and which arise from the interaction of a harmonic linear wave field with a body located within that field. The scattering potential is solved for the body when it is held fixed, and may be used to determine the exciting force acting on the body due to the wave action. The radiating potential, wherein the potential is found for a moving body in the absence of incident waves, is commonly resolved into components in phase with the body acceleration and the body velocity, and gives rise to the added-mass and radiation damping terms.

A number of commercial software codes have been developed to implement BEM to determine the hydrodynamic parameters of user-generated geometries. Such codes include WAMIT, Aquaplus, Aqwa and WADAM, all of which are

TABLE I: The Available BEM Solvers and their Characteristics

BEM solver	Frequency domain	Time domain	Open source	Usage [%]*	Arrays*	Point Absorber*	OWC*	OWSC*	Other*	Time domain simulation*	Multiple modes*
WAMIT [2]	✓	✗	✗	80.5%	15.2%	39.3 %	24.2 %	21.2 %	21.2 %	44.5%	51.5 %
NEMOH [3]	✓	✗	✓	19.5%	12.5%	62.5 %	0 %	37.5 %	25 %	25 %	75%
AQWA [4]	✓	✗	✗	22%	11.1%	11.1 %	22.2%	11.1 %	44.4 %	55.5 %	77.7 %
Aquaplus [5]	✓	✗	✗	9.8%	25 %	25 %	0 %	50 %	50 %	100 %	50 %
ACHIL3D [6]	✗	✓	✗	4.9%	50 %	100 %	0 %	0 %	0 %	100 %	0%
WADAM [7]	✓	✗	✗	7.3%	66 %	33 %	33 %	0%	33%	100%	66%

* Statistics are based on the publications in [1], where 14.2% of the publications referenced a BEM solver.

frequency domain solvers, and ACHIL3D, which is a time domain solver. In 2014, the École Centrale de Nantes released NEMOH, an open-source frequency domain BEM solver. These codes allow to users with low expertise in the fundamental mathematical basis underpinning the software codes to obtain the frequency-domain coefficients of a hydrodynamic problem.

III. Methodology

In this section, the rationale behind the choice of which commercial BEM solver is to be compared with NEMOH is discussed. Next, the motivation for the choice of geometries to be examined is explained, before the criteria by which the comparison between the two BEM solvers is performed are described.

A. Choice of BEM solver

Based on the results of keyword searches, 14.2% of the papers in [1] explicitly reference one or more BEM software tools. When only those papers within the wave energy tracks are considered, the figure of papers referencing a BEM solver rises to 37.5%. While some independent work has previously been performed to compare the results obtained for the analysis of cargo ships using NEMOH and WAMIT in the frequency domain, [8], the aim of the present paper is to evaluate the usefulness of NEMOH to the wave energy community. To this end, a survey of [1] was undertaken and the results are presented in Table I. This survey used keyword searches to identify when a BEM solver (or solvers) was referenced in a paper, and also the specific BEM solver(s) referenced. Each paper was then investigated to determine the nature of the WEC(s) analysed. Next, the papers were examined to determine if time-domain modelling was performed. Finally, each paper was scrutinised to determine if a single degree of freedom, or multiple degrees of freedom (or multiple, interacting bodies each acting in a single degree of freedom), were modelled. One, unsurprising, result of this survey, which can be seen from Table I, is that WAMIT was the most frequently referenced BEM code in [1], referred to in over 80% of papers which cited a BEM solver. As such, WAMIT may be taken as the de facto standard. The demonstrable widespread use of WAMIT by the wave energy community is the rationale behind taking WAMIT as the benchmark to which NEMOH is compared.

B. Device selection

Once the decision was taken to use WAMIT as the benchmark to which NEMOH would be compared, the next decision to be made concerned which types of WECs, and hence geometries, to consider. This decision was informed by the results in Table I, by the geometries typically examined by the research group to which the authors are affiliated and also by devices commonly presented in the literature. This paper considers four different types of WEC for which real-world exemplars exist: a submerged axisymmetric point absorber (SAPA), a two-body point absorber (2BPA), an oscillating surge wave converter (OSWC), and a floating oscillating water column (OWC). Further, two configurations for the two-body point absorber are analysed. The form of both two-body point absorbers is identical with the single difference that one configuration includes a heave damping plate (Spar_{wdp}), while the second configuration does not include a damping plate ($\text{Spar}_{\text{nodp}}$). The main characteristics of the geometries used in the present comparison are given in Table II.

TABLE II: Main Geometric Characteristics* of the WECs used for the Comparison.

Device type	Realistic WEC	Principal dimensions	Water depth
SAPA	CETO [9]	$R = 8.5$ $H = 6$ $H_{FS} = -2$	20
2BPA	OPT [10]	$R_{F_{out}} = 4.75$ $R_{F_{in}} = 3$ $T_F = 2.25$ $R_S = 2.5$ $R_{dp} = 5.9$ $T_S = 35$	∞
OSWC	Oyster [11]	$W = 2$ $L = 20$ $H = 12$	13
OWC	Sparbuoy [12]	$R_{out} = 3$ $R_{in} = 2$ $T = 10$	∞

* In the *Principal dimensions* column, R is the radius, H the height, H_{FS} the distance from the top of the device to the free-surface, T the draft, W the width and L the length. In addition, subscripts $_{out}$ and $_{in}$ indicate the outside and inner radius, respectively, and $_F$, $_S$ and $_{dp}$ refer to the float, spar cylinder and the damping plate of the 2BPA, respectively. All the dimensions in the table are shown in metres.

Heaving devices such as point absorbers, oscillating surge wave converters and oscillating water columns make up over 90% of the 166 proposed WECs examined by Babarit [13].

The generic geometries examined here, while based on specific devices, nonetheless represent a good cross section of the geometries that are common in the field of wave energy.

C. Outcome selection

The final decision to be made concerned which parameters to compare. Based on the perceived usage of BEM solvers within the wave energy community, see Table I, the following parameters are considered to compare the results obtained from the two solvers in both the frequency domain and the time domain:

- Exciting force (N)
- Added mass (kg)
- Radiation damping (Ns/m)
- Impulse response function (IRF).

Due to the large number of result generated for the present study, which includes hydrodynamic coefficients and exciting forces for all the devices listed in Table II, and, in some instances, which operate in multiple degrees of freedom resulting in cross coupling terms, illustrating all the results in graph form is impractical. Furthermore, discrepancies between NEMOH and WAMIT may arise due to diverse causes, but such discrepancies do not necessarily indicate a failure on the part of NEMOH. Thus, it is not possible to show the correspondence between the results obtained from the two solvers by using a single similarity measure. Therefore, the comparison between NEMOH and WAMIT is shown by using three metrics based on two different measures, namely the cross-correlation and root mean square (RMS) ratio.

The cross-correlation measure compares two series as a function of the displacement of one relative to the other, and shows the similarity of the two signals for all the possible relative positions, as one signal is stepped over a second signal, and is used in pattern recognition. For two series comprising n elements, the cross-correlation of the two signals results in a vector of correlations with $2n$ values. Each value in the cross correlation vector lies between -1 and 1, where 1 means a perfect positive correlation exists between the two signals, 0 indicates no correlation between the two signals and -1 shows a perfect negative correlation exists between the two signals.

For the present study, where curves of hydrodynamic coefficients as function of frequency obtained from NEMOH and WAMIT are compared, two values from the cross correlation vector are considered. The first value of interest is the correlation when the two signals are relatively displaced so that the corresponding frequencies of the two signals align. This value is termed *XC*. The second value is the maximum correlation value, termed *maxXC*, which may not occur when the two signals are relatively displaced, i.e. frequencies align. In this way, *XC* shows the similarity of the shape of the two curves from NEMOH and WAMIT when the frequencies are aligned, while the *maxXC* highlights the best similarity of the shape of the curves, correcting for any frequency shift.

An example of when the maximum correlation between the results from NEMOH and WAMIT does not occur when the frequencies of the two curves align arises, for example, when a system includes a moonpool. The resonant frequency of the moonpool calculated by NEMOH and the corresponding value calculated by WAMIT can be slightly different. As a consequence, the *XC* value is significantly low, whereas the *maxXC* value will be high. The low value of *XC* does not necessarily demonstrate poor performance of NEMOH in such a case. If there is no such frequency shift, *XC* and *maxXC* values are identical.

A third metric is required however, as the *XC* and *maxXC* values only show the similarity of the two curves in terms of their shape. These metrics give no indication as to the relative amplitudes of the two signals. Therefore, the RMS ratio (*RMSr*) is used. This ratio is obtained by dividing the RMS of the frequency dependent results obtained for a parameter from WAMIT by the RMS of the corresponding results obtained from NEMOH. In this case, *RMSr* value of 1 means the RMS of the results from NEMOH is identical to the RMS of the corresponding results from WAMIT. A *RMSr* value above 1 means the RMS of the results from NEMOH are lower than the RMS of the corresponding results from WAMIT and a *RMSr* values below 1 indicates that the RMS of the NEMOH results are lower than the WAMIT equivalent.

Note that this study is limited to first order forces and does not consider second order forces, such as second order drift forces. Furthermore, computation time taken by each solver is considered. In order to make a fair comparison between the results from the two solvers, the number of panels used for each geometry with the two solvers is kept as similar as possible.

The authors have no direct affiliations to any organisation associated with the BEM solvers referenced in this paper, and have approached this work from an entirely independent standpoint. The decision was taken not to attempt to modify any BEM codes from the standard distributions, and that no third party software, such as CAD modellers would be employed, although the usefulness of the results obtained from the two solvers with respect to post-processors is considered. It is the aim of the authors that the results be akin to those that would be produced by an intelligent user, rather than an expert on any specific BEM code.

Both NEMOH and WAMIT comprise three main routines, which are designed to run consecutively: the pre-processor, the processor and the post-processor. The capabilities of NEMOH and WAMIT are compared for each routine in the following sections.

IV. Pre-processor

In the pre-processor, the input files created by the user are read by the application and the mesh is prepared for the simulation. Inputs include environmental values, such as sea water density, water depth, wave frequencies or wave directions; or body conditions, like the number of bodies and degrees of freedom (DoFs) to be analysed or the number of panels of which the mesh comprises. It is important to note that parameters such as gravity or sea water density are not required in WAMIT, since WAMIT generates non-dimensional results.

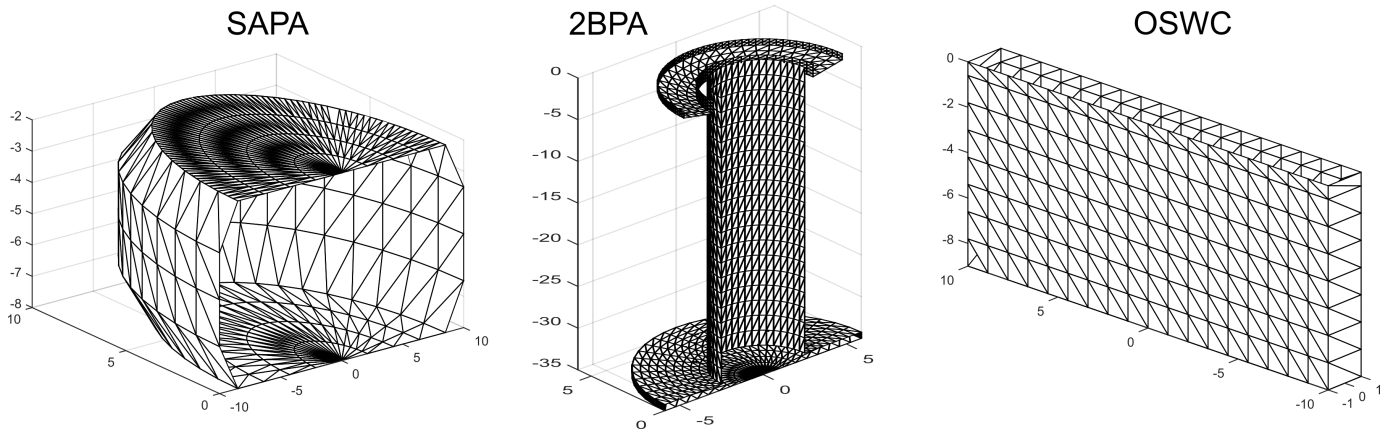

Fig. 1: The low-order meshes for the SAPA, 2BPA and OSWC devices.

Two characteristics of the pre-processor routine are compared herein: user-friendliness, and mesh generation capabilities.

A. User-friendliness

WAMIT requires multiple input files to run a simulation. The typical number of input files required for the simplest simulation is five:

- *config.wam* specifies various parameters and options, including irregular frequency removal flag or high/low order mesh option. The WAMIT user manual recommends the use of a second configuration file;
- *SIM.cfg* can include most of the parameters defined in the *config.wam* file. A number of exceptions exists, such as the parameters which controls the number of cores to be used during the parallelisation.
- *SIM.pot* defines the environmental parameters (except gravity and sea water density), calls the mesh file and defines the number of DoFs and the origin of the body-fixed coordinate system;
- *SIM.gdf* describes the wetted surface of the geometry to be analysed; and
- *SIM.frc* includes the flags for the output results, indicating which results are required from the simulation; and the information of the body, such as the mass matrix, the centre of gravity and can include external damping and stiffness values (for simulations with moorings, for example).

Note that *SIM* refers to the name of the simulation, which is defined by the user and does not have to be the same for all the files. Therefore, one more file (*fnames.wam*) that includes the names of the *SIM.cfg*, *SIM.pot* and *SIM.frc* files may be used.

Preparation of the equivalent information in NEMOH is significantly simpler, where a single input file (*Nemoh.cal*) includes all the necessary parameters for the simulation. Furthermore, *ID.dat*, which includes the working directory, and *input.txt* need to be located in the working folder, together with the file *Nemoh.cal*.

In addition, NEMOH provides a Matlab wrapper (*Nemoh.m*) to run the simulations, which makes the process considerably more user-friendly for the users who are familiar with Matlab. Apart from the wrapper, Matlab routines are also provided for meshing, as described in Section IV-B, and post-processing, as explained in Section VI.

It should be noted that the Matlab wrapper was used to obtain the results for this paper.

1) Manual & Test-cases: An important difference between WAMIT and NEMOH is the documentation provided by the developers. While WAMIT provides a comprehensive user manual describing each required input file and option of the software, along with all output generated by the software, NEMOH only offers a short description of the code with limited instructions to use the software. In addition, WAMIT provides 25 different test cases, with several sub-cases, that cover many of the different possibilities WAMIT offers. The user manual includes an appendix where all the test cases are explained. To the best knowledge of the authors, NEMOH does not offer such a benchmark for different cases. The authors of the present paper believe that the lack of a complete manual and basic test cases is one of the significant weaknesses of NEMOH.

B. Mesh generation

Consider now mesh generation for use as input for the two solvers. WAMIT does not include any embedded mesh generator. However, it provides a set of subroutines that generate different pre-defined geometries, such as spheres, rectangular barges, torus or even a "floating production ship offloading ". However, any geometry that is not included in the subroutines, requires an external software to generate the mesh to be used in WAMIT.

WAMIT can use two fundamentally different geometry discretisation methods: low- and high-order. The low order method can be considered as the standard discretisation method, where the geometry of the body is divided into a number of flat quadrilateral panels. In the high-order method, in contrast, the body is divided into a number of patches, which, in turn, are divided into panels. Such panels in the high-order method do not have to be necessarily flat panels, as is the case for the low-order method, and can have the curvature the geometry

surface requires to precisely represent the body. B-splines of different orders are use to represent the surfaces.

The solution of the velocity potential is approximated by using constant values on each panel in the low-order method, which results in a piecewise representation of the velocity potential. In contrast, velocity potential is represented by continuous B-splines in the high-order method, providing a more accurate solution.

NEMOH can only offer the low-order method, where all the body geometries are represented by means of flat quadrilateral panels, such as those shown in Figure 1. A low-order mesh generated in WAMIT would be very similar, if not identical, to the low-order mesh generated in NEMOH.

However, NEMOH includes two Matlab functions to generate axisymmetric (*axiMesh.m*) and non-axisymmetric meshes (*Mesh.m*). Axisymmetric meshes can be generated very easily by providing only a few points of the contour of the geometry. In addition, the user can also decide radial and vertical discretisation of the mesh for higher accuracy. For non-axisymmetric geometries, the user needs to define the coordinates (x, y and z) for the four nodes of each panel, in the correct order so that the normal vector points towards the fluid, and generate a matrix with all the coordinates to be used as the input for the *Mesh.m* function. A limitation of the Matlab mesh generator functions in NEMOH is the number of panels, or more specifically, the number of nodes that may be used. Matlab displays a 'sever error' when geometries of over 10000 nodes are defined.

One relevant difference between WAMIT and NEMOH meshes is the symmetry plane. While WAMIT allows 2 symmetry planes (x0z and y0z), NEMOH only allows one plane (x0z), which may affect the computational requirements of a simulation.

An important issue with meshes is the format of the file. In fact, very few software can export mesh files with the *.gdf* or *.mar* extension WAMIT and NEMOH require, respectively. Therefore, WAMIT users can only use the predefined subroutines or specific software, such as *Multisurf* to generate their meshes, while NEMOH users can generate their own meshes using the Matlab functions. In addition, NEMOH includes Matlab functions to convert mesh files, i.e. *nemoh2wamit_01.m* that converts NEMOH meshes into *.gdf* format or the *GDFmesh.m* function that directly reads *.gdf* meshes.

Finally, even though it is not directly related to any of the solvers, the external software *Meshmagick* [14] can be employed to convert mesh files from one format to another. The current version of Meshmagick supports *.stl* format, which is a common option of CAD software, and mesh formats for most of the hydrodynamic solvers, such as NEMOH, WAMIT, Diodore or Hydrostar, and also visualisation software like Tecplot or Paraview. That way, mesh files can be generated using the majority of CAD software packages and convert them into the require format using *Meshmagick*.

V. Processor

The processor is the routine where the solver runs. In this case, the processor solves the boundary value problem for each case defined in the pre-processing part and generates output files containing the results. Therefore, the processing capabilities are analysed by comparing the hydrodynamic coefficients described in Section III-C and the computational requirements to generate those results.

Results of the comparison between the hydrodynamic coefficients are shown in Table III, using the three measures described in Section III. A colour code with three colours (green, orange and red) highlights the agreement between NEMOH and WAMIT. Green colour indicates a cross-correlation or RMSr of between 0.9 and 1.1. Orange indicates a cross-correlation or RMSr between 0.8 and 0.9 and 1.1 and 1.2. Red indicates any values outside these ranges.

It should be noted that the version 2 of the NEMOH solver, v2_03 is used in the present study, since the new version, v3, with more capabilities is currently under development.

A. Hydrodynamic coefficients

The hydrodynamic coefficients from WAMIT and NEMOH were obtained for the four WECs described in Table II, including the two spar cylinder options for the 2BPA. The mesh used in the simulations in WAMIT and NEMOH is identical for the SAPA, the 2BPA in both configurations studied and the OSWC, for which the mesh generated in NEMOH is converted into *.gdf* files to be used in WAMIT. In the case of the OWC, due to the incompatibility of the meshes used in the different modelling options, the authors have used meshes with similar number of panels, as explained in Section V-A4.

1) Submerged axisymmetric point absorber: SAPAs deployed in shallow/intermediate water, such as the CETO device [9], mainly operate in three DoFs: surge, heave and pitch. Therefore, added-mass, radiation damping and excitation force coefficients for these three DoFs are compared in Table III, including the coupling between surge and pitch and heave and pitch.

Results from the two solvers are so similar that the *XC* and *maxXC* values are very close to 1, which would illustrate a perfect match, for all the DoFs. RMSr ratios also show values very close to one and lower than 1 for most of the DoFs, which means the amplitude for NEMOH is larger in general. The main differences appear at the peaks of the coefficients, where NEMOH coefficients are slightly larger. Results are almost identical for the rest of the curve, as illustrated in Figure 2.

2) Two-body point absorber: The 2BPAs analysed here, which are similar to the Ocean Power Technology (OPT) [10] device, operate in deep water and consist of a torus float and a central spar cylinder with or without damping plate, and use the same DoFs as the SAPA to extract energy from ocean waves. The motivation for including a two-body system is to analyse the capability of the BEM solvers to represent the interaction between the two bodies. Further, the OPT device is of particular interest because of the damping plate of the central spar buoy, which may be an issue for NEMOH if represented by thin elements. In addition, the presence of the moonpool between the float and the spar increases the complexity of the analysis. Although it is well known that

TABLE III: Comparison of the hydrodynamic coefficients obtained in WAMIT and NEMOH for the four device types.

Devices		Added-mass				Radiation damping				Excitation force			Added-mass at infinite freq.			IRF			
		s	h	p	s-p	s	h	p	s-p	s	h	p	s	h	p	s	h	p	
SAPA		0.9998	0.9995	1.0000	0.9993	0.9993	0.9997	0.9998	0.9988	0.9998	0.9999	0.9996	N/A	N/A	N/A	0.9993	0.9998	0.9998	*XC*
		0.9998	0.9995	1.0000	0.9993	0.9993	0.9997	0.9998	0.9988	0.9998	0.9999	0.9996	N/A	N/A	N/A	0.9993	0.9998	0.9998	*maxXC*
		0.9358	0.9750	0.9568	0.9234	0.9233	0.9556	0.9626	0.8994	0.9821	0.9661	0.9654	0.9418	1.0121	0.9635	0.9238	0.9558	0.9626	*RMSr*
2BPA	Float	0.8996	0.9682	0.8655	0.7862	0.2657	0.7790	0.3949	0.2394	0.7348	0.9915	0.9105	N/A	N/A	N/A	0.8773	0.9609	0.8848	
		0.8996	0.9682	0.9499	0.8539	0.9991	0.9879	0.9945	0.9994	0.9948	0.9915	0.9987	N/A	N/A	N/A	0.9393	0.9609	0.9316	
		1.0210	0.9888	0.9197	0.9166	1.0681	0.9374	1.2165	1.1916	0.8524	0.9994	0.9582	2.9897	0.9864	1.0349	1.0836	0.9468	1.1514	
	$Spar_{nodp}$	0.9733	1.0000	0.8636	0.8561	0.2888	0.9995	0.2850	0.2870	0.8544	1.0000	0.7992	N/A	N/A	N/A	0.8715	0.9684	0.8716	
		0.9733	1.0000	0.8819	0.8781	0.9985	0.9995	0.9986	0.9985	0.9963	1.0000	0.9963	N/A	N/A	N/A	0.9479	0.9684	0.9496	
		0.9786	1.0348	0.8941	0.8881	1.1253	0.9760	1.1025	1.1107	0.9124	0.9996	0.8788	1.0043	1.0348	1.1039	1.1111	0.9765	1.0898	
	$Float\text{-}Spar_{nodp}$	0.8495	0.9990	0.7687	0.2754	0.2494	0.9900	0.3294	0.2492	N/A	N/A	N/A	N/A	N/A	N/A	0.8644	0.9823	0.8638	
		0.8495	0.9990	0.8701	0.8518	0.9995	0.9900	0.9963	0.9995	N/A	N/A	N/A	N/A	N/A	N/A	0.9376	0.9823	0.9444	
		0.9338	0.9898	0.7807	0.9269	1.0997	0.9827	1.1266	1.0855	N/A	N/A	N/A	1.0722	1.2073	1.1286	1.1286	0.9842	1.0922	
	$Spar_{wdp}$	0.8443	1.0000	0.3284	0.2270	0.1233	0.9242	0.1169	0.1198	0.8001	0.9995	0.6994	N/A	N/A	N/A	0.8885	0.9454	0.8865	
		0.9803	1.0000	0.9904	0.9923	0.9907	0.9343	0.9902	0.9905	0.9942	0.9995	0.9948	N/A	N/A	N/A	0.9403	0.9454	0.9411	
		0.9956	1.0404	1.0278	1.0241	1.2428	0.5858	1.2374	1.2345	0.9646	0.9954	0.9499	0.9879	1.0404	1.0244	1.2457	0.6072	1.2423	
	$Float\text{-}Spar_{wdp}$	0.0374	0.8127	0.1459	0.2216	0.0634	0.3933	0.1612	0.0645	N/A	N/A	N/A	N/A	N/A	N/A	0.8503	0.3166	0.9056	
		0.9939	0.8127	0.9927	0.9943	0.9736	0.3933	0.9965	0.9735	N/A	N/A	N/A	N/A	N/A	N/A	0.9498	0.4594	0.9441	
		1.1240	0.8255	0.9398	1.1177	1.2801	0.4474	1.1397	1.2705	N/A	N/A	N/A	-6.310	0.4537	1.0076	1.3202	0.4110	1.1337	
OSWC		N/A	N/A	0.9902	N/A	N/A	N/A	0.9779	N/A	N/A	N/A	0.9853	N/A	N/A	N/A	N/A	N/A	0.9994	
		N/A	N/A	0.9902	N/A	N/A	N/A	0.9938	N/A	N/A	N/A	0.9927	N/A	N/A	N/A	N/A	N/A	0.9994	
		N/A	N/A	1.0493	N/A	N/A	N/A	1.0753	N/A	N/A	N/A	1.0713	N/A	N/A	0.9935	N/A	N/A	1.0207	
OWC	Buoy	N/A	0.9996	N/A	N/A	N/A	0.9618	N/A	N/A	N/A	0.9978	N/A	N/A	N/A	N/A	N/A	0.9858	N/A	
		N/A	0.9996	N/A	N/A	N/A	0.9618	N/A	N/A	N/A	0.9978	N/A	N/A	N/A	N/A	N/A	0.9858	N/A	
		N/A	0.9395	N/A	N/A	N/A	0.8668	N/A	N/A	N/A	0.9860	N/A	N/A	0.9426	N/A	N/A	0.9005	N/A	
	Free-surface (thin disk)	N/A	0.4494	N/A	N/A	N/A	0.1698	N/A	N/A	N/A	0.5470	N/A	N/A	N/A	N/A	N/A	0.1916	N/A	
		N/A	0.4494	N/A	N/A	N/A	0.3973	N/A	N/A	N/A	0.7167	N/A	N/A	N/A	N/A	N/A	0.1995	N/A	
		N/A	0.8179	N/A	N/A	N/A	0.0011	N/A	N/A	N/A	0.4285	N/A	N/A	2.5453	N/A	N/A	0.0012	N/A	
	Free-surface (FC)	N/A	0.9998	N/A	N/A	N/A	0.8719	N/A	N/A	N/A	0.8990	N/A	N/A	N/A	N/A	N/A	0.9997	N/A	
		N/A	0.9998	N/A	N/A	N/A	0.8837	N/A	N/A	N/A	0.8990	N/A	N/A	N/A	N/A	N/A	0.9997	N/A	
		N/A	1.1823	N/A	N/A	N/A	1.2972	N/A	N/A	N/A	1.2324	N/A	N/A	1.0804	N/A	N/A	1.2681	N/A	

* s, h and p refer to surge, heave and pitch modes, respectively, and s-p corresponds to the coupling between surge and pitch.

** Results for the added-mass column in the case of the OWC free-surface modelled via the FC technique are obtained using the total inertia term that includes the added-mass and the mass of the cylinder.

***N/A is used to show the corresponding measure is not applicable in that case.

linear potential flow solvers cannot accurately capture the physics of the flow in such small water gaps, it is informative to compare the results between WAMIT and NEMOH when modelling this gap.

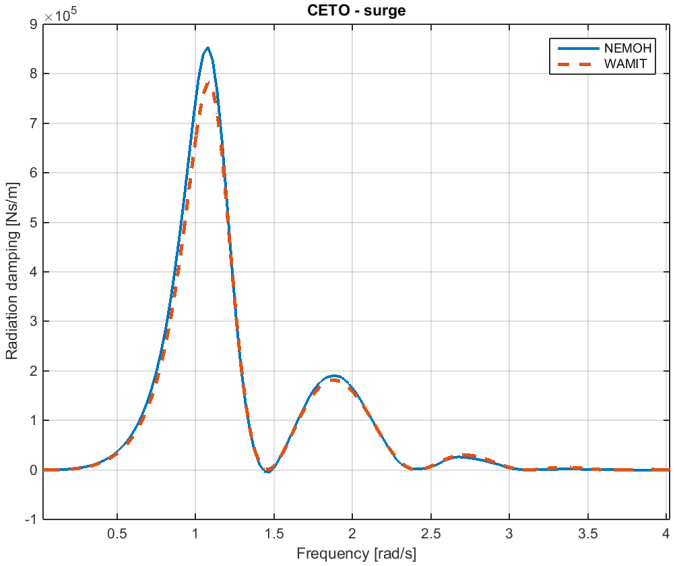

Fig. 2: Radiation damping for surge mode of the SAPA device

Table III shows the similarity metrics described for the two 2BPA options, with and without the damping plate, with the results divided into 5 different sections: the float, which shows identical results in both cases; the $\text{Spar}_{\text{nodp}}$; the interactions between the float and the $\text{Spar}_{\text{nodp}}$; the Spar_{wdp}; and the interactions between the float and the Spar_{wdp}. Similarity measures show good agreement between NEMOH and WAMIT for the 2BPA without the damping plate (including the float and the spar cylinder).

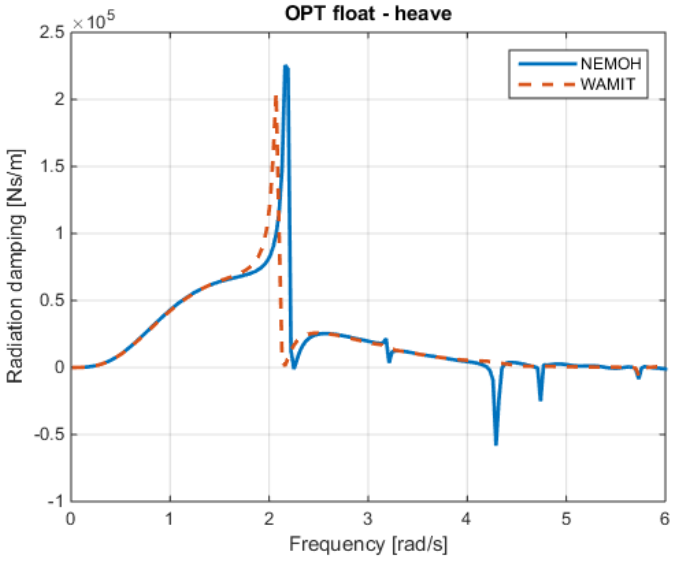

Fig. 3: Radiation damping for heave mode of the 2BPA float

The mayor difference between NEMOH and WAMIT for the 2BPA is the frequency shift, showing higher *maxXC* than *XC* for most of the coefficients. Figure, 3 illustrates, however, that NEMOH provides good results for the 2BPA float and the fact that the moonpool frequency lies at a slightly higher frequency in NEMOH should not be taken as an issue of the NEMOH solver. In addition, one can note irregular spikes at high frequencies (around 3.2, 4.3 and 4.8 rad/s, in this case) in the NEMOH curve, which are not present in the WAMIT curve. These spikes are irregular frequencies, which arise due to a fundamental error in the formulation of the BEM solver, regardless of type of solver. WAMIT results do not show such spikes, because WAMIT includes an option to remove irregular frequencies. NEMOH also offers a preliminary option to remove them, but it is not fully implemented at this time, so it has not been included in this study.

With respect to the 2BPA where the spar cylinder includes a damping plate, results are similar for the added-mass, where the frequency shift is the main source for differences. However, radiation damping coefficients for different DoFs appear to be problematic in this case, as illustrated in Figure 4.

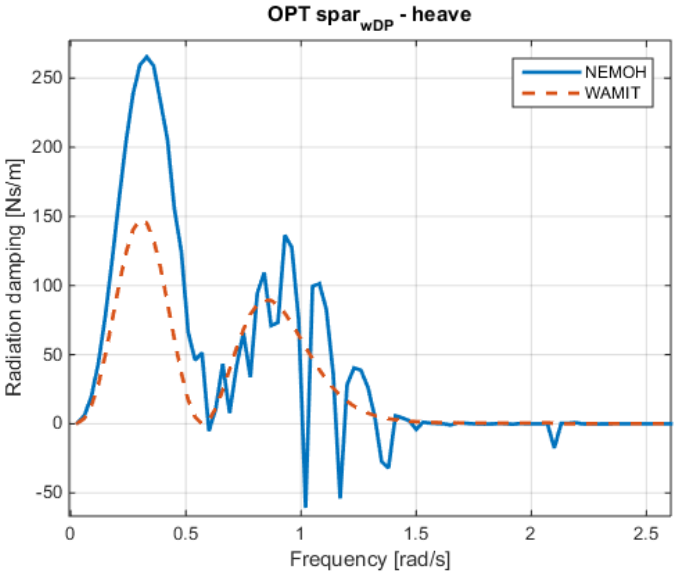

Fig. 4: Radiation damping for heave mode of the 2BPA spar cylinder with damping plate

In the 2BPA with damping plate case, the spar cylinder includes a relatively thin element at the bottom, which appears to be the source of odd spikes in the damping curve at relatively low frequencies. The authors have considered different sources of the issue with the damping plate, such as the water depth or the mesh convergence. However, while the degree to each spikes occur in the radiation damping curve varies as these potential sources for error are varied, the issue always occurs in the case of a 2BPA including a damping plate. Figure 5 illustrates the results of that mesh convergence study, demonstrating the issue is not panel-dependent. Although the spikes appear to be similar to the irregular frequencies shown in Figure 3, NEMOH developers suggest in the forum that they can arise *"due to approximations in tabulations of the Green function"*, an issue which will be considered in the future version (v3).

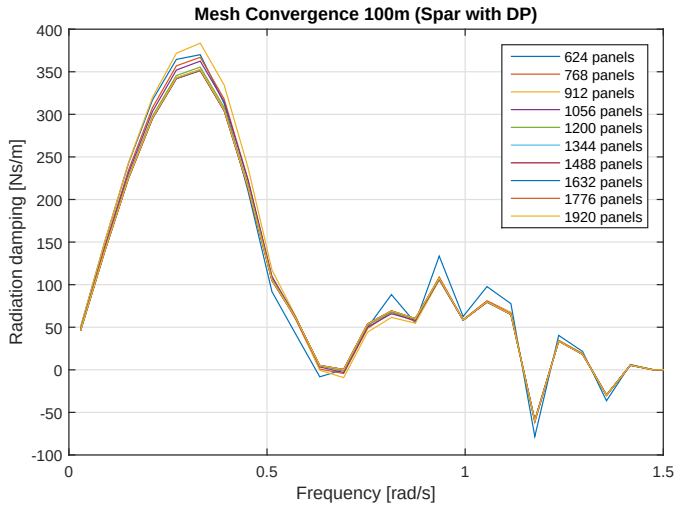

Fig. 5: Mesh convergence study of the spar cylinder with a damping plate

3) Oscillating surge wave converter: The motivation for including an OSWC, such as the Oyster device by Aquamarine Power Ltd. [11], arises from the fundamental difference in the mode of operation of such a device when compared to any point absorber. OSWCs only use the pitch mode to extract energy from ocean waves, so only pitch coefficients are studied.

The agreement of the two solvers is clearly shown in Table III, where all the measures show that hydrodynamic coefficients match almost perfectly. Similarly to the SAPA device, the only difference between the coefficients obtained from NEMOH and WAMIT are the magnitudes of the peak values, which are always slightly lower in NEMOH.

4) Oscillating water column: An OWC device is also interesting for this comparison, as it involves a crucial aspect for BEM solvers: modelling of the free-surface elevation of a moonpool. Modelling OWC devices using BEM codes, using either WAMIT or NEMOH, is especially challenging due to the very particular behaviour of the free-surface in the OWC chamber, where nonlinear effects appear to be particularly relevant [15]. The traditional method of modelling the free-surface inside the OWC chamber is by using an infinitely thin massless disk (lid) to represent the free-surface [16], referred to as the thin disk method henceforth. However, WAMIT provides a number of methods to model OWC devices, including a generalised mode that considers the free-surface at the moonpool as a extension of the body surface and a new patch is assigned to this extension in the higher order method. Generalised modes are then applied to the patch and the motion of the moonpool is modelled as the heave motion of the the additional patch.

The only way the free-surface inside the chamber can be modelled in NEMOH is using the traditional method, modelling a two-body system where the lid is modelled as a thin cylinder, as illustrated in Figure 6 (a). Thus, in order to provide a fair comparison between the two solvers while showing the full capabilities of both solvers, the use of two-body system models in NEMOH and WAMIT, plus a third case using the generalised modes in WAMIT, are compared.

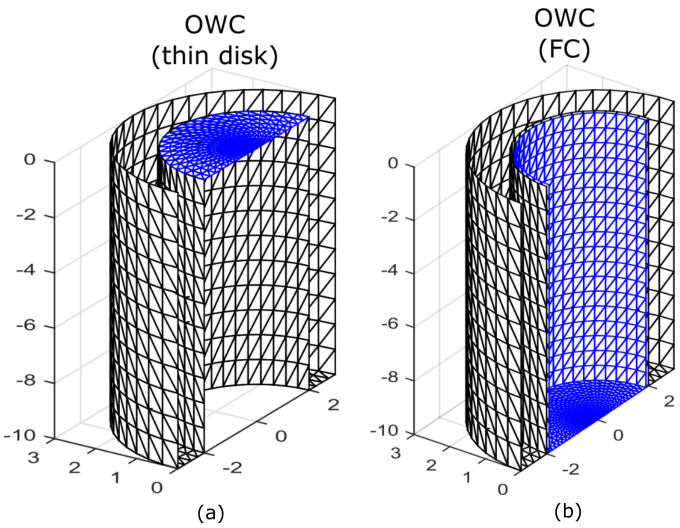

Fig. 6: Meshes of the two options to model OWC devices.

With respect to the meshes used in the different cases, since a single body is analysed in the generalised mode, it is not possible to use the same mesh in the three cases. However, mesh files with very similar number of panels have been generated in NEMOH, so that results from the different cases provide a fair comparison.

Results shown in Table III show good agreement for the OWC buoy, which is similar to the OPT float, and so good agreement was to be expected. However, when modelling the free-surface of the moonpool using the thin disk method, NEMOH fails to reproduce hydrodynamic coefficients. While added-mass and excitation force coefficients in NEMOH are different from the WAMIT coefficients, these results appear to be reasonably realistic. In contrast, the radiation damping generated in NEMOH is clearly wrong, showing negative values, as illustrated in Figure 7, which is completely unrealistic.

Results from WAMIT using the two different modelling techniques based on the thin disk method show very similar results for low frequencies, but diverge for higher frequencies, as shown in Figure 7.

NEMOH developers warn in the website that NEMOH "*may not work*" when modelling OWCs and recognise mesh convergence as "*challenging*". Therefore, a mesh convergence study of the disk that models the free-surface was carried out. Nevertheless, radiation damping of the simulation using the finest mesh also fails.

Another, alternative method to model the free-surface is suggested in [17], where a cylinder of the same length as the water column is used to represent the water column. This method is referred to as the full cylinder method (FC) henceforth, and the mesh generated to apply the FC method is illustrated in Figure 6 (b). Results given by WAMIT using the FC method are identical to the results obtained using the thin disk method except for the added-mass. However, when the total inertial term, which is the sum of the mass of the water

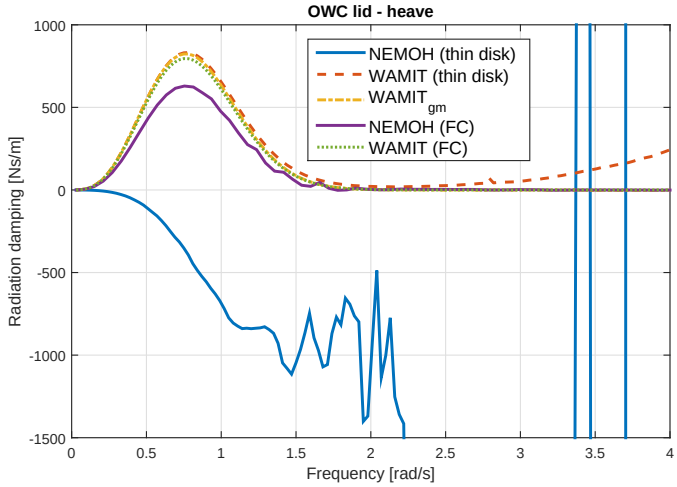

Fig. 7: Radiation damping for the heave mode of the moonpool free-surface of the OWC for NEMOH and WAMIT, using the three different methods: thin disk, FC and generalised modes ($WAMIT_{gm}$)

in the water column and the added-mass of the cylinder, is considered, identical results are obtained in WAMIT for the two different two-body modelling techniques.

In addition, because no thin elements are used when modelling the OWC via the FC technique, NEMOH provides what appears to be realistic results for all the hydrodynamic coefficients, including radiation damping, as shown in Figure 7. Results in Table III for the FC modelling technique show that results from WAMIT and NEMOH are very similar, where a frequency offset between the WAMIT and NEMOH curves seems to be the only difference, as shown in the RMSr in Table III and in Figure 7. It should be noted that the similarity values corresponding to the added-mass in the FC case are obtained by comparing the total inertia term. Therefore, FC appears to be an effective modelling technique, which is particularly convenient for NEMOH users.

B. Computational requirements

The computational requirements of the processor are studied for the different cases analysed in Section V-A. One of the main advantages of WAMIT in this respect, is the option to parallelise the simulation over the cores of the PC. In addition, WAMIT includes an option to set the maximum RAM memory to be used by the solver, so that the remaining RAM is available for other applications.

In order to provide a fair comparison, simulations have been carried out in a 64bit laptop with 8Gb RAM, 8 cores (4 real and 4 virtual) and an *Intel Core i5-5200U* processor of 2.20 Ghz CPU. Since WAMIT can run simulation in parallel, 4 cores have been used in WAMIT simulations, and only one in NEMOH.

Results comparing the computational requirements of the two solvers are given in Table IV, where NEMOH proves to be significantly slower than WAMIT, up to 17 times slower for the case with the higher number of panels.

TABLE IV: Simulation time for the different cases in WAMIT and NEMOH

	# freq.	# modes	# panels	NEMOH	WAMIT
SAPA	136	1+3*	430	160.69s	22.57s
2BPA	202	1+6*	285+1104**	5992.18s	356.33s
OSWC	335	1+1*	330	53.19s	15.29s
OWC	200	1+2*	656+240**	1199.15s	117.76s***
	200	1+2*	656+816**	2516.87s	141.64s***

* #diffraction problems + #radiation problems, from #bodies + #DoFs)
** Number of panels in 2-body systems : #panels$_{body1}$ + #panels$_{body2}$.
*** Simulation time in WAMIT using the generalised mode is significantly lower: 49.48s.

VI. Post-processor

The post-processing routine refers to the treatment of the results obtained in the processing routine. In this regard, a number of third party software tools exist which may be used to post-process the results from BEM solvers. Some of these tools, such as ProteusDS and WECSim, will accept the output of both WAMIT and NEMOH as input, while others, for example, Inwave, which integrates the NEMOH code, will only accept the output of NEMOH, or only the output of WAMIT, such as HydroDyn. However, as both NEMOH and WAMIT generate results in text format, the authors consider it a trivial task to transform the output of one of these solvers into the form of the output of the other solver, and, as such, in this regard, neither solver has a great advantage over the other.

However, post-processing also provides a framework to carry out further operations using the results from the processing stage, such as calculating time domain parameters, like added-mass at the infinite frequency or the IRF.

A. Time-domain coefficients

The added-mass at the infinite frequency (A_∞) may be directly given by the solver in WAMIT. The IRF can be obtained from the WAMIT frequency domain results using the *F2T.exe* provided by WAMIT, for which the time vector needs to be defined.

In NEMOH, the time-domain coefficients are calculated using the external *FD2TD.m* function, for which the first output is A_∞ and the second is the IRF. The IRF can also be calculated by activating the flag in the *Nemoh.cal* file, and in both cases the time vector for the IRF needs to be provided.

Because frequency-domain coefficients for the SAPA, the 2BPA without the damping plate and the OSWC show very good agreement, it is not surprise that the agreement for the time-domain coefficients also showed good agreement.

In the case of the 2BPA with a damping plate, the discrepancies in the added-mass at the infinite frequency are considerably higher than for the added-mass curve, which suggests that the irregular frequencies at high frequencies may have a strong negative impact. Similar conclusion can be drawn for IRFs, but this time the odd spikes in the radiation damping cause the discrepancies rather than the irregular frequencies. Since neither the odd spikes nor the irregular

frequencies are real effects, one could remove them manually from the NEMOH curves, which may positively modify the time-domain coefficients.

In the case of the OWC, the discrepancies in time-domain coefficients are to be expected, given the frequency-domain coefficients obtained in NEMOH.

VII. Discussion

The ability of the open-source BEM solver NEMOH to reproduce results obtained using the commercial BEM solver WAMIT, in the context of wave energy converters has been reviewed in this paper. Some of the aspects covered in this paper, together with several other issues and suggestions, are identified in the NEMOH users' and developers' forums, although such a validation of the NEMOH code against an established software, focusing on geometries suitable for wave energy, has never been presented before either in the literature or the forum.

With regards to the pre-processor, NEMOH is a highly user-friendly software, in no small due to the Matlab wrapper, which makes running the NEMOH solver significantly easier for the novice when compared to using WAMIT. In addition, NEMOH includes Matlab functions to generate mesh files for axisymmetric and non-axisymmetric geometries, although a limitation for the number nodes (10000 nodes) appears to exist. However, it should be noted that 10000 nodes is already quite high, and a greater number of nodes would only be required in very specific and complex cases. Matlab functions to convert WAMIT mesh files to a format suitable for NEMOH are available, while NEMOH has the ability to use low-order WAMIT *.gdf* mesh files as input. In contrast, WAMIT only includes certain subroutines for specific geometries. The main weakness of NEMOH is the lack of documentation in terms of a comprehensive manual and representative test cases, which are provided by WAMIT.

NEMOH shows good overall agreement for many cases providing added-mass, radiation damping and excitation force coefficients. Results are particularly good for the SAPA, the 2BPA with no damping plate, the OSWC and the OWC when using the FC technique. Poor results are only found when using thin elements in the model, as demonstrated by the 2BPA with the damping plate and the moonpool free-surface of the OWC. The issue with thin elements is well documented in the NEMOH forums and the manual, so these poor results were expected. Indeed, a NEMOH work package has been created specifically to address the issue of thin elements.

In addition, the irregular frequency removal option in NEMOH is still not fully implemented, which means odd spikes arise in the results at high frequencies for floating bodies in general. Such irregular frequency removal option is available in WAMIT. Further, WAMIT also includes the special "dipole panel" to model thin elements, which allows to model zero-thickness elements.

With respect to the computational requirements, simulation times required by NEMOH and presented in TableIV are consistently higher than those required by WAMIT. This is, in no small part, due to the parallelisation option included in WAMIT. Although not included in the present study, since NEMOH offers the Matlab wrapper to run the BEM solver, one could modify the Matlab scripts to use the parallelisation toolbox in Matlab to parallelise the job over the different cores of the PC.

The post-processing capabilities compared in the present study for NEMOH and WAMIT appear to be very similar, where coefficients that are used for time-domain simulations, A_∞ and IRFs, show very good agreement for all the cases where frequency-domain results are accurately reproduced.

All files used in the generation of the results presented herein will be made available on the COER website .

Acknowledgement

This material is based upon works supported by the Science Foundation Ireland under Grant No. 13/IA/1886 and the Sustainable Energy Authority of Ireland under Grant No. OCN/00031.

References

[1] *Proc. 11th European Wave and Tidal Energy Conference (Nantes, France, September 2015)*. Technical Committee of the European Wave and Tidal Energy Conference, 2015.

[2] M. WAMIT Inc., *WAMIT v7.0 manual*, 2013.

[3] A. Babarit and G. Delhommeau, "Theoretical and numerical aspects of the open source bem solver nemoh," in *11th European Wave and Tidal Energy Conference (EWTEC2015)*, 2015.

[4] A. W. ANSYS Inc., *AQWA manual Release 15.0*, 2013.

[5] G. Delhommeau, "Seakeeping codes aquadyn and aquaplus," in *Proc. of the 19th WEGEMT School, Numerical Simulation of Hydrodynamics:Ships and Offshore Structures*, 1993.

[6] A. Babarit, *Achil3D v2.011 User Manual.*, Laboratoire de Mécanique des Fluides CNRS, Ecole Central de Nantes, 2010.

[7] DNV-GL, "Frequency domain hydrodynamic analysis of stationary vessels - wadam." (Last accessed 07/04/2017). [Online]. Available: https://www.dnvgl.com/services/frequency-domain-hydrodynamic-analysis-of-stationary-vessels-/wadam-2412

[8] G. Parisella and T. Gourlay, "Comparison of open-source code nemoh with wamit for cargo ship motions in shallow water," Centre for Marine Science and Technology, Curtin University, Tech. Rep. 2016-23, October 2016.

[9] J. Fiévez and T. Sawyer, "Lessons learned from building and operating a grid connected wave energy plant," in *Proceedings of the 11th European Wave and Tidal Energy Conference, Nantes*, 2015.

[10] M. Mekhiche and K. A. Edwards, "Ocean power technologies powerbuoy®: System-level design, development and validation methodology," in *Proceedings of the 2nd Marine Energy Technology Symposium, METS, Seattle (WA)*, 2014.

[11] M. Folley, T. Whittaker, and J. v. Hoff, "The design of small seabed-mounted bottom-hinged wave energy converter," in *Procedings of 7th European Wave and Tidal Energy Conf. (EWTEC), Porto*, 2007.

[12] A. F. Falcão, J. C. Henriques, and J. J. Cândido, "Dynamics and optimization of the owc spar buoy wave energy converter," *Renewable energy*, vol. 48, pp. 369–381, 2012.

[13] A. Babarit, "A database of capture width ratio of wave energy converters," *Renewable Energy*, vol. 80, pp. 610 – 628, 2015.

[14] F. Buisson and F. Rongére, "Meshmagick." [Online]. Available: http://130.66.47.2/redmine/projects/meshmagick/wiki/Wiki

[15] M. Penalba, G. Giorgi, and J. V. Ringwood, "Mathematical modelling of wave energy converters: a review of nonlinear approaches," *Renewable and Sustainable Energy Reviews*, vol. 78, pp. 1188–1207, 2017.

[16] D. Evans, "The oscillating water column wave-energy device," *IMA Journal of Applied Mathematics*, vol. 22, no. 4, pp. 423–433, 1978.

[17] W. Sheng, R. Alcorn, and A. Lewis, "Hydrodynamics of oscillating water column wave energy converters," *Renew 2014*, 2014.